Biogeosciences Discuss., 10, 17117–17144, 2013
www.biogeosciences-discuss.net/10/17117/2013/
doi:10.5194/bgd-10-17117-2013

Biogeosciences Discussions
Open Access

Revisiting the disappearance of terrestrial dissolved organic matter in the ocean: a $\delta^{13}C$ study

K. Lalonde[1], A. V. Vähätalo[2,*], and Y. Gélinas[1]

[1]GEOTOP and Department of Chemistry and Biochemistry, Concordia University Montreal, Quebec, Canada
[2]Department of Bio- and Environmental Science, University of Helsinki, Finland
[*]now at: Biological and Environmental Science, University of Jyväskylä, Finland

Received: 11 October 2013 – Accepted: 16 October 2013 – Published: 1 November 2013

Correspondence to: Y. Gélinas (yves.gelinas@concordia.ca)

Published by Copernicus Publications on behalf of the European Geosciences Union.

Abstract

Organic carbon (OC) depleted in ^{13}C is a widely used tracer for terrestrial OM in aquatic systems. Photochemical reactions can however change $\delta^{13}C$ of dissolved organic carbon (DOC) when chromophoric, aromatic-rich terrestrial OC is selectively mineralized. We assessed the robustness of the $\delta^{13}C$ signature of DOC ($\delta^{13}C_{DOC}$) as a tracer for terrestrial OM by estimating its change during the photobleaching of chromophoric DOM (CDOM) from ten large rivers. These rivers cumulatively account for approximately 1/3 of the world's freshwater discharge to the global ocean. Photobleaching of CDOM by simulated solar radiation was associated with the photochemical mineralization of 16 to 43 % of the DOC and, by preferentially removing compounds depleted in ^{13}C, caused a 1 to 2.9 ‰ enrichment in $\delta^{13}C$ in the residual DOC. Such solar radiation-induced photochemical isotopic shift biases the calculations of terrestrial OM discharge in coastal oceans towards the marine end-member. Shifts in terrestrial $\delta^{13}C_{DOC}$ should be taken into account when constraining the terrestrial end-member in global calculation of terrestrially derived DOM in the world ocean.

1 Introduction

The oceanic dissolved organic carbon (DOC) pool is large (662×10^{15} g OC; Hansell et al., 2009), representing a quantity of carbon that is approximately equal to that of carbon dioxide in the atmosphere and terrestrial plant biomass (Hedges, 2002). The turnover of OC within the oceanic reservoir is supported by marine and continental photosynthesis, with vascular plant detritus and soil organic matter mainly transported to the ocean by continental erosion and riverine discharge. Apportioning these sources is challenging since oceanic DOM has a complex, highly altered structure, consisting mainly of relatively small molecules in fairly uniform and very dilute concentrations (Benner et al., 1997). Most evidence points to a nearly purely marine origin for oceanic DOM, as indicated by (1) its marine-like $\delta^{13}C$ signature (Bauer, 2002; Druffel et al.,

BGD
10, 17117–17144, 2013

1992); (2) the low abundance or absence of terrestrially-derived molecular biomarkers within the DOM pool (Opsahl and Benner, 1997; Ogawa and Tanoue, 2003) and (3) the compositional and optical dissimilarities between riverine and seawater DOM (Blough and Del Vecchio, 2002).

Though oceanic DOM is predominantly marine-like, there is evidence that a small yet non-negligible component of DOM has a terrestrial origin. Studies using resin and ultrafiltration-isolated lignin molecules have shown that the terrestrial component varies between 4 and 10 % of the isolated fractions of DOM (Opsahl and Benner, 1997; Meyers-Schulte and Hedges, 1986). These are likely underestimations since solar radiation-induced photochemical reactions break apart large aromatic-rich molecules like lignin, tannin and cutin (Hernes and Benner, 2003; Dittmar et al., 2007; Vähätalo et al., 1999) into molecular fragments that can be difficult to isolate from seawater's salty matrix (too hydrophilic for hydrophobic resins or too small for ultrafiltration) and identify as terrestrial compounds using current analytical methods (Rossel et al., 2013).

Optical parameters (absorbance and fluorescence) that are specific to riverine DOM are also particularly susceptible to photochemical transformation since the light-absorbing, chromophoric riverine DOM components are selectively removed upon exposure to UV radiation in a process called photobleaching (Blough and Del Vecchio, 2002; Helms et al., 2008). Photobleaching of terrestrial DOM is associated with the photochemical mineralization of DOC, acting as a partial sink for terrestrial DOC (Moran et al., 2000). The residual non-mineralized fraction of photobleached terrestrial DOM has optical properties that are similar to marine DOM; its terrestrial origin cannot be recognized using the currently available optical methods (Helms et al., 2008; Vähätalo and Wetzel, 2008; Spencer et al., 2009).

Stable isotopes of carbon are typically used to trace terrestrial DOM in coastal, estuarine and marine systems since they are thought to incur little to no change in their isotopic signature upon partial OC degradation (Druffel et al., 1992; Raymond and Bauer, 2001a, b; Maher and Eyre, 2011). Photochemical transformations have however been shown to shift the stable isotope signature of DOC derived from a plant leachate or

BGD
10, 17117–17144, 2013

collected from a humic lake and three different rivers of different size (Osburn et al., 2001; Vähätalo and Wetzel, 2008; Spencer et al., 2009; Opsahl and Zepp, 2001).

Direct (complete mineralization to CO_2) or indirect (increase in the bioavailability of DOC followed by rapid biological mineralization to CO_2) photochemical transformations are important pathways in the mineralization of terrestrial DOM (Miller and Zepp, 1995; Spencer et al., 2009; Mopper et al., 1991). Together, these processes can possibly explain the removal of up to 80 % of riverine DOC (Obernosterer and Benner, 2004). However the remaining, non-photoreactive and biologically recalcitrant DOC, representing > 20 % of the global riverine input, is still large enough to support more than half the steady-state turnover of oceanic DOC (0.1×10^{15} gC yr^{-1}) (Williams and Druffel, 1987). Thus it remains puzzling that terrestrial DOM accounts for such a small percentage of oceanic DOM. It is possible that riverine DOM remains in oceanic waters but is altered beyond recognition through photodegradation and bacterial relabeling during passage in the microbial loop, allowing it to escape from the analytical windows of traditional measurement methods.

In the present study, we study the effect of photochemical and microbial transformations on isotopic signatures of riverine DOC. We measured the potential isotopic shifts of DOC δ^{13}C during (1) abiotic photochemical mineralization of a portion of the DOC pool to CO_2 and other purgeable organics and inorganics associated with a nearly complete photochemical decomposition of riverine chromophoric DOM (CDOM) and (2) the bacterial mineralization of biologically labile DOC produced during the photochemical transformation of DOC. The riverine DOC was collected from ten major rivers, cumulatively representing 1/3 of the world's freshwater discharge and 28 % of the marine input of continental DOC (Cauwet, 2002) allowing us to appropriately constrain the continental end-member. We calculate the difference in the apportionment between the marine and terrestrial DOC components using the $\delta^{13}C_{DOC}$ signature of before and after the irradiation treatment. We show how a photochemical shift in $\delta^{13}C_{DOC}$ signatures influences the use of ^{13}C isotopes for quantifying terrigenous DOC in the oceans and how

BGD
10, 17117–17144, 2013

to account for these changes when quantifying the terrestrial component of oceanic DOC.

2 Materials and methods

2.1 Riverine samples

The rivers selected in this study are responsible for 33 % and 28 % of freshwater discharge and DOC flux to the ocean, respectively (Table 1). They drain 25 % of land area in a wide range of ecosystems and climates on five continents (Milliman and Farnsworth, 2011). The selected rivers provide a representative end-member of riverine discharge in the ocean and a predicting tool for the behavior of riverine DOM in oceanic waters.

A water sample was collected from each river in 10 L polyethylene containers (cleaned with detergent, rinsed with acid and Milli-Q water) during the season of high discharge. The polyethylene containers were cleaned at the University of Helsinki and shipped to the local operators at each river (see list in Acknowledgments). The containers were filled in the center of the stream by direct immersion below the surface from a boat, except for the Mississippi and St. Lawrence Rivers where near surface water (about 3 m below the surface) was collected with Niskin bottles and directly transferred to the polyethylene containers. All samples were immediately placed in a box to shield the water from sun and artificial light. They were left unfiltered/unkilled upon shipment and storage at the University of Helsinki (the time lag between sampling and measurement was between 80–390 days) so that the most labile fraction of the DOC (L-DOC) in all samples was decomposed prior to the measurement reported in this study (see below). The same water samples used here have been also examined for the concentration of dissolved black carbon and the contribution of iron to CDOM (Jaffé et al., 2013; Xiao et al., 2013). Additional samples from the St. Lawrence River were collected at the same time as the polyethylene container, filtered on-board (pre-combusted GF/F

BGD
10, 17117–17144, 2013

filters, 0.7 µm nominal pore size), acidified with ultrapure HCl to a pH < 2, and stored in pre-combusted glass vials.

2.2 Irradiation experiment followed by a bioassay

All samples were sterile filtered (0.2 µm, Sartobran 300, Sartorius) and separated into two batches of duplicates: one set of irradiated samples to be compared to a batch of dark control samples. Irradiated samples were placed in clean and combusted (> 2 h, 450 °C) UV-transparent 750 mL quartz vials fitted with ground glass stoppers. A headspace corresponding to 10 % of the vial internal volume was filled with O_2 gas, and replenished after 4 days of irradiation to support complete oxidation of the UV-sensitive DOM fraction (Vähätalo and Wetzel, 2008). The samples were placed horizontally 1 cm below the surface of water on a stainless steel grid in a flow-through pool of tap water regulated to 24.5 ± 1.0 °C. They were exposed for 10 days to simulated solar radiation adjusted to a power that mimics the global mean of a half-year UV dose of solar radiation. The simulated solar radiation was generated using a metal halide lamp (Thorn OQ 1000, UK) and fluorescent tubes (UVA-340, Q-Lab Corp., Canada), and measured with a Macam SR 991 spectroradiometer in air 2 cm above the quartz flasks. The spectral irradiance of the artificial light source comprised the photochemically active part of UV radiation present in natural sunlight but excluded any environmentally non-relevant short-wavelength UV radiation absent from solar radiation incident to the ocean (Fig. 1b). Dark controls were treated in the same way (sterile filtered, but kept at 21.6 ± 2.1 °C in the dark). We preserved samples with ultrapure HCl (pH < 2) for DOC concentration and $\delta^{13}C$ measurements at the beginning and end of the irradiation.

In order to quantify the microbial mineralization of labile DOC produced during the abiotic photochemical transformation of riverine DOM, we introduced a microbial inoculum into the irradiated and the dark control samples. Each sample received KH_2PO_4 to the final concentration of 133 P µg L^{-1} and unfiltered water from its corresponding river (1 % vol vol^{-1}) as a source of phosphorus nutrient and microbial inoculum, respectively. These bioassay flasks contained an air headspace and were incubated in the dark at

BGD
10, 17117–17144, 2013

22.0 ± 0.5 °C. After 28 days of incubation, the samples were filtered and preserved with HCl for the measurement of DOC concentration and its $\delta^{13}C$ signature as explained above.

Note that any biologically labile organic compound present in the original water samples was degraded during sample shipment and storage through microbial processes that do not affect $\delta^{13}C$ signature of DOM to a significant extent (Obernosterer and Benner, 2004; Stutter et al., 2013; Lu et al., 2013). Since biologically labile riverine DOM (L-DOM), which does not contribute to the global oceanic DOM reservoir, is degraded on hourly to daily time scales, the DOM fraction that was used at the start of the irradiation experiment corresponds to non-biologically labile DOM (NL-DOM). NL-DOM comprises semi-labile and refractory DOM, which have degradation rates on the order of years to centuries (Obernosterer and Benner, 2004). Note also that we report changes in the concentration and $\delta^{13}C_{DOC}$ of NL-DOC during a two-stage process: (1) the complete bleaching of NL-CDOM under sterile conditions followed by (2) the biodegradation of the residual non-photosensitive organic compounds. In natural systems, these two NL-DOM degradation pathways take place simultaneously rather than consecutively. Our experimental design thus probably overestimates the relative importance of photochemical degradation since in natural environment, there is competition for DOC substrates that are both bioavailable and photodegradable during daily light/dark cycles. However, as photobleaching leads to significant changes in $\delta^{13}C$ signatures while biodegradation does not (Table 1), we focused mostly on $\delta^{13}C_{DOC}$ shifts occurring during photobleaching when interpreting the fate NL-DOM in the ocean.

2.3 High-temperature catalytic oxidation DOC-IRMS measurements

A combustion total organic carbon (TOC) analyzer (OI Analytical Model 1010, College Station, TX) was modified to reduce background contamination from atmospheric CO_2 by replacing all gas-permeable polytetrafluoroethylene (PTFE) tubing with polyether ether ketone (PEEK) tubing. Ultra-high purity oxygen carrier gas and platinum-coated silica particles (5 % Pt (w/w)) were used for combustion of samples. Prior to analysis,

BGD
10, 17117–17144, 2013

the instrument furnace was kept at temperature of 680 °C, under clean O_2 for several hours, followed by the injection of a total of 100 blanks, ensuring low background CO_2 levels. Trapping the background CO_2 without injecting a liquid sample on the combustion column produced a peak corresponding to 0.18 µgC. The results obtained for the samples were corrected for this low background contribution.

The TOC analyzer was interfaced to an Isoprime isotope ratio mass spectrometer (IRMS) through a Graden instrument chemical CO_2 trap, which allows quantitative recovery of CO_2 while switching the carrier gas from oxygen to ultra-high purity helium. Each sample injection therefore provided both the DOC concentration (by NDIR on the TOC analyzer and by the measured voltage on the IRMS) and $\delta^{13}C$ isotopic composition. The correlation coefficient between the NDIR and voltage-derived concentrations was > 0.98. Dry certified sucrose standard ($\delta^{13}C = -10.45 \pm 0.03$ ‰) from the International Atomic Energy Agency (IAEA-CH-6) and β-alanine (Sigma-Aldrich, -26.18 ± 0.33 ‰ standardized in-house against several certified materials by elemental analysis-IRMS) were dissolved in ultrapure water and used as calibration and reference compounds.

The injection volume was adjusted to 750 µL, generating enough CO_2 for high precision concentration and isotopic measurements without compromising combustion efficiency. Twin vials of each sample were run in either duplicate or triplicate, yielding standard deviations of ≤ 0.15 mg L^{-1} and ≤ 0.3 ‰ for concentration and isotopic measurements, respectively. Isotope data is reported with standard notation ($\delta^{13}C$) in parts per thousand (‰) relative to the Pee Dee Belemnite standard.

3 Results and discussion

3.1 Riverine NL-DOC concentrations and $\delta^{13}C_{NL\text{-}DOC}$ signatures

The measured NL-DOC concentrations (mean ± SD) in the rivers examined ranged from 0.79 ± 0.03 mg L^{-1} (Ganges-Brahmaputra) to 5.94 ± 0.13 mg L^{-1} (Congo) with

BGD
10, 17117–17144, 2013

a yearly discharge-weighted average of $3.60 \pm 0.1\,mg\,L^{-1}$ (Table 1) for all rivers. The $\delta^{13}C_{NL\text{-}DOC}$ signatures (mean ± SD) ranged from -28.99 ± 0.17 ‰ (Amazon) to -25.98 ± 0.21 ‰ (Mekong) with a yearly discharge-weighted average of -28.07 ± 0.20 ‰ (Table 1). These weighed average NL-DOC concentrations and $\delta^{13}C_{NL\text{-}DOC}$ values could be used as a first-order estimate for terrestrial riverine DOC discharged in the ocean. Additional studies are however needed to improve the accuracy of this estimate by taking into account the quantitatively important rivers not sampled in this project, as well as potential seasonal and inter-annual variability in NL-DOC concentrations and $\delta^{13}C_{NL\text{-}DOC}$ signatures.

The concentration of NL-DOC and $\delta^{13}C_{NL\text{-}DOC}$ signatures reported in Table 1 do not include the biologically labile fraction of DOC (L-DOC), which was biodegraded during the shipping and storage of samples. L-DOC was not measured directly in the other rivers but corresponds to the fraction of riverine DOC that is rapidly consumed by microbes, therefore too reactive to contribute to the oceanic reservoir of DOC. In the St. Lawrence River, the L-DOC fraction accounted for 19 ± 1 % ($n = 3$) of total DOC (measured on separate aliquots collected on the same day), consistent with previously reported estimates of 13 and 28 % in lacustrine and swamp settings (Obernosterer and Benner, 2004) or 22 ± 12 % of total DOC in the coastal ocean (Lønborg and Álvarez-Salgado, 2012).

The $\delta^{13}C_{DOC}$ signatures measured for total DOC and NL-DOC in the St. Lawrence River were -26.45 ± 0.43 ‰ and -26.13 ± 0.16 ‰, respectively (Table 1). These results suggest that the removal of L-DOC by biodegradation does not alter $\delta^{13}C_{DOC}$ signatures, in agreement with several earlier studies (Obernosterer and Benner, 2004; Stutter et al., 2013; Lu et al., 2013).

3.2 Photochemical shift in $\delta^{13}C_{NL\text{-}DOC}$ signatures

Our irradiation experiment was designed to simulate the photochemical transformations of riverine DOM upon photobleaching of CDOM in the mixed layer of the coastal

BGD
10, 17117–17144, 2013

ocean (Figs. 1 and 2). Simulated solar radiation most effectively targets chromophores that absorb in the regions of the spectrum that overlap with the most intense irradiance bands (Fig. 1a). In all samples, the simulated radiation effectively resulted in the virtually complete loss of absorption at a wavelength of 350 nm (Fig. 2), which parallels the disappearance of the terrestrial optical signal. Photobleaching of riverine CDOM by sunlight in the coastal ocean has also been shown in previous irradiation experiments or field studies measuring CDOM in situ or by remote sensing (Vodacek et al., 1995; Vähätalo and Wetzel, 2008; Nelson et al., 2010).

The photobleaching of CDOM was concomitant to the photochemical mineralization of NL-DOC, as illustrated in Fig. 3b and Table 1. The loss of NL-DOC by photomineralization ranged from 16 % (St. Lawrence) to 43 % (Congo), with an average of 36 % for the all rivers examined (Table 1). No well-stained bacteria were found in the irradiated samples by epifluorescence microscopy, indicating that the partial mineralization of NL-DOC (to DIC), as well as any structural, spectral and isotopic modifications of the NL-DOC pool are incurred due to a purely abiotic photochemical process. In contrast to the irradiated samples, the absorption by CDOM or the concentration of NL-DOC did not change in the dark control samples during the ten-day time irradiations (Figs. 2 and 3b).

Photochemical reactions specifically target certain molecular moieties/types, therefore causing an overall change in the chemical composition of DOM. Indeed, photodegradation occurs at a high rate when the concentration of chromophoric moieties that have high absorptivity in the blue and UV region of the spectrum (high $a_{\lambda<350\,\mathrm{nm}}$) is high (Mopper and Kieber, 2002). This chromophoric DOM component constitutes the major portion of the organic carbon in many lakes, rivers, and even some coastal waters, and is structurally similar to soil humics, with a characteristic brown color (Hedges and Oades, 1997; Blough and Del Vecchio, 2002). It is composed of a mixture of lignocellulose-derived polyelectrolytes that result mainly from the decay of terrestrial vegetation and aquatic detritus (Gonsior et al., 2008; Dittmar et al., 2007).

BGD
10, 17117–17144, 2013

A removal process specifically targeting these molecules causes a severe molecular fractionation in the DOM pool, which is reflected by an isotopic shift in $\delta^{13}C_{DOC\text{-}NL}$. We observe a 0.48 ‰ (Yangtse) to 2.29 ‰ (Parana) enrichment in photodegraded NL-DOC. The average riverine $\delta^{13}C_{NL\text{-}DOC}$ shifts from −28.07 ‰ to −26.57 ‰ (Table 1, Fig. 4). Recent studies have also highlighted similar shifts towards heavier δ^{13}C-DOC values upon photochemical mineralization of DOC. These shifts averaged 6 ‰ for plant leachate, 1.2 ‰ for a humic lake, 0.7 ‰ for the Altamaha River, 1.6 ‰ for the Satilla River, and 3.1 ‰ for the Congo River (Lu et al., 2013; Osburn et al., 2001; Vähätalo and Wetzel, 2008; Spencer et al., 2009; Opsahl and Zepp, 2001). The photochemical isotopic shift measured in this study for the Congo River was not as pronounced as reported by Spencer et al. (2009) for the same river (1.7 ‰ vs. 3.1 ‰, respectively). This apparent disagreement may be related to differences in the temperature and the source of irradiation, but more likely to different initial δ^{13}C-DOC signatures in the two studies (−29.2, ‰ this study vs. −27.1 ‰ for Spencer et al., 2009); the δ^{13}C signature of photobleached NL-DOC was similar in both studies (−26.2 ‰ vs. −26.3 ‰).

Noteworthy, this $\delta^{13}C_{DOC\text{-}NL}$ enrichment is seen consistently for all riverine samples. The ^{13}C-enrichment of UV-resistant NL-DOC occurs due to the mineralization of ^{13}C-depleted NL-DOC components, varying between −25.75 ‰ and −33.92 ‰ and averaging −30.85 ‰ (calculated by isotopic mass balance for the 10 studied rivers). Naturally photosynthesized ^{13}C-depleted components of terrestrial plants include, amongst others, macromolecular aromatic compounds such as lignin, tannins and cutins (4–7 ‰ depletion in comparison to bulk plant material, Hayes, 2001; Goni et al., 2005). The preferential photooxidative breakdown of these compounds can therefore explain why over 80 % of the molecules remaining in the deep ocean consist largely of small molecularly uncharacterized, oxygenated DOM compounds that bear little or no resemblance to the parent molecules (Benner et al., 1997). Photobleaching simultaneously explains the three main changes in DOM that make riverine DOM appear deceivingly more marine in nature: (1) the decrease in average molecular size; (2) the reduction in

BGD
10, 17117–17144, 2013

the abundance of aromatic/unsaturated functionalities; and (3) the overall enrichment in $\delta^{13}C$.

3.3 Does biodegradation shift the $\delta^{13}C$ signature of terrestrial NL-DOC?

Photochemical enhancement of DOM bioavailability has previously been shown to be an important factor in the alteration of estuarine and coastal heterotrophy (Zepp, 2005; Chin-Leo and Benner, 1992; Vähätalo et al., 2011). We therefore extended our irradiation experiment with a bioassay and examined whether microbial mineralization of phototransformed NL-DOC results in any further shift in $\delta^{13}C_{NL\text{-}DOC}$. After the addition of indigenous microbes to the irradiated sample, the decrease in NL-DOC concentrations ranged between 21.9 % (Ganges-Brahmaputra) and 37.7 % (Congo) (average of 32.6 ± 2.4 %) during the 28 day bioassay (Fig. 3b and Table 1). Microbial consumption in the dark control samples was negligible (5 ± 7 % of NL-DOC; data not shown). Our irradiation experiment clearly indicates that photochemical transformations do not only mineralize NL-DOC directly to DIC, but also produce labile photoproducts in a magnitude similar to DIC (Table 1). Our results are in agreement with earlier studies, which have found out that labile photoproducts are a quantitatively important component of photochemical transformation of DOC (Vähätalo et al., 2003; Pullin et al., 2004; Obernosterer and Benner, 2004; Aarnos et al., 2012). The mineralization of these labile photoproducts was not associated to an isotopic shift (average shift of 0.02 ± 0.15 ‰ during the bioassay, Table 1), in agreement with the negligible of isotopic shifts during the biodegradation of the L-DOC fraction of the St. Lawrence River sample and with data reported in earlier studies (Obernosterer and Benner, 2004; Stutter et al., 2013; Lu et al., 2013).

BGD
10, 17117–17144, 2013

3.4 Relationship between NL-DOM photochemical susceptibility and $\delta^{13}C_{NL\text{-}DOC}$

The susceptibility of ^{13}C-poor NL-DOM materials towards photochemical losses is reflected by the increased proportion of UV-resistant NL-DOC in riverine systems with enriched $\delta^{13}C_{NL\text{-}DOC}$ (Fig. 5). ^{14}C-enriched materials also tend to be more photochemically susceptible, therefore it is possible that photochemical mineralization is implicated in the preservation of ^{14}C-aged (Beaupré and Druffel, 2012), ^{13}C-enriched (this study) DOC in the ocean. It is interesting to consider the use of riverine $\delta^{13}C$ signatures as a predictive tool for estimating the maximum potential photochemical and bacterial removal of riverine NL-DOC in the ocean. Assuming (i) that the NL-DOC fraction is composed of two pools of organic matter (a UV-resistant and microbially recalcitrant pool of dissolved organic compounds (R-DOC), and second pool of compounds that are mineralized upon photobleaching followed by microbial incubation), and (ii) that these two pools have contrasting average $\delta^{13}C$ signatures (R-DOC is more ^{13}C-enriched), the fractional contribution of the two pools can be estimated directly from the model II linear regression shown in Fig. 5b (($\delta^{13}C_{NL\text{-}DOC}$ + 32.35)/12.31), where the measured fractional contribution of the UV/microbially resistant DOC pool (R-DOC) is plotted against $\delta^{13}C_{NL\text{-}DOC}$. The high correlation coefficient (0.925) and the relatively low standard error on the slope (± 1.69) and y-intercept (± 0.73) allow extrapolating the regression to fractional contributions of 0 and 1, which helps constrain the range of possible $\delta^{13}C$ signatures for the NL-DOC pool. According to this simple model, the lower limit corresponds to the average $\delta^{13}C$ signature of the pool of organic compounds that are mineralized following the photobleaching and incubation (-32.35 ± 0.73 ‰), while the higher limit gives the theoretical signature of pure R-DOC (-20.04 ± 0.42 ‰). Noteworthy, the estimated $\delta^{13}C$ constraint for the R-DOC pool is very close to the signature of purely marine DOC (−20 ‰, see below).

The samples most prone to photobleaching are therefore the most ^{13}C-depleted and also contain the largest fraction of directly photodegradable compounds (absorb

BGD
10, 17117–17144, 2013

most strongly at wavelengths > 350 nm ($aCDOM_{350}$); Fig. 5a). The most degradable samples therefore likely contain freshest terrestrial NL-DOM (less photobleached) and were likely collected in rivers with low residence time and/or efficient shielding from light (DOM self-shielding, high particulate loads and/or forested banks). The Congo River is an exception to the $\delta^{13}C$ trend, experiencing the highest NL-DOC losses of all rivers but displaying relatively enriched values. This outlier could result from a relatively high discharge of C4 vascular plant material compared to the other rivers (these plants have similar optical properties and molecular characteristics to those of C3 vascular plants, however displaying a more enriched $\delta^{13}C$ values). The $\delta^{13}C$ signature of total DOC was found to vary greatly between seasons (−30.6 to −25.8 ‰) in one of the main tributaries of the Congo River, which was explained by a complex hydrological cycle and multiple sources of DOC with contrasting $\delta^{13}C$ signatures, including C4 plants (Bouillon et al., 2012).

3.5 The effect of photochemical $\delta^{13}C$-shift when calculating the contribution of terrestrial NL-DOC to the oceanic DOC reservoir

The highest exposure of DOM to sunlight occurs at the mouth of estuaries and river plumes, where fresh riverine waters are spread into a thin surface layer or are mixed into denser, more translucent saline waters. Our irradiation and incubation experiment predicts the ultimate removal of approximately 2/3 (range of 42 to 81 %) of the original NL-DOC pool during its passage through the sunlit waters of these mixing zones as well as in ocean margin and mid-ocean regions (Table 1, Fig. 1). The exact half-life of riverine CDOM depends on the depth of the photolytic zone (transparency relating to particulate load and DOM shielding), as well as the intensity of sunlight and other climatic/environmental considerations. Previous studies report CDOM half-lives at approximately 1.5 yr in irradiated seawater (Miller and Zepp, 1995) or 1000 to 4200 yr in the mixed world ocean (Mopper et al., 1991). CDOM is broken down into non-chromophoric molecules (through DIC and low molecular weight DOM production) that are further degraded by bacteria, leaving behind an altered, UV-transparent/resistant

BGD
10, 17117–17144, 2013

and microbially recalcitrant DOC (R-DOC) component, consistent with the nearly complete absence of chromophoric molecules in the mid-ocean and deep bottom waters (Benner et al., 1997; Blough and Del Vecchio, 2002). Assuming that the proportions of the R-DOC and NL-DOC components are similar to those of other rivers worldwide (i.e., 19 to 52 % of the NL-DOC fraction is R-DOC), we extrapolate that between 0.034 and 0.128×10^{15} gC yr^{-1} of the total global riverine NL-DOC export (range of $0.18 - 0.22 \times 10^{15}$ gC yr^{-1}, corresponding to between 72 and 87 % of the global riverine DOC export of 0.25×10^{15} gC yr^{-1}; Cauwet, 2002) resists photobleaching/microbial decay and possibly contributes to the slow cycling DOC pool in the ocean. Though it represents only a small fraction of the total riverine DOC export, this yearly contribution of UV-resistant material equates to more than half the estimated turnover of DOC in the ocean (Williams and Druffel, 1987).

Photochemical degradation shifts $\delta^{13}C_{DOC}$ signatures toward marine values, thus leading to underestimations of the terrestrial component and complicating the use of $\delta^{13}C_{DOC}$ for tracking terrigenous DOC in the oceans. The problem is exacerbated by the fact that the $\delta^{13}C$ signatures of both the marine and terrestrial DOC components of oceanic waters are not well constrained (Bauer, 2002). The marine DOC end-member (−20 ‰) is difficult to measure directly, but can be inferred from the C3 fixation pathway having a theoretical 19 ‰ fractionation from dissolved DIC in the ocean (Bauer, 2002; Yu et al., 2008). Constraining the stable isotopic signature of the riverine end-member is more difficult and requires that processes that potentially shift the $\delta^{13}C$ values be adequately considered. As the importance of photobleaching (both direct photobleaching and bacterial mineralization caused by a photochemically induced increase in bioavailability) as a sink for terrestrial DOC in the ocean is being increasingly recognized, it is important to account for the isotopic shifts associated to this removal pathway in particular to appropriately constrain the $\delta^{13}C$ signature of the terrestrial DOC component that mixes with oceanic DOC (Table 2). Using a two end-member isotopic mixing system and the $\delta^{13}C$ values of the marine and terrestrial end-members (and assuming that the microbial degradation of L-DOM does not affect $\delta^{13}C$ signatures significantly),

BGD
10, 17117–17144, 2013

it is therefore possible to calculate the fraction (f) of terrestrial NL-DOC in mid-ocean and deep ocean water samples (Eq. 1):

$$\delta^{13}C_{measured} = f_{marine}\delta^{13}C_{marine} + f_{riverine}\delta^{13}C_{riverine} \quad (1)$$

Table 2 shows the calculated proportions of the marine and terrestrial end-members in different oceanic samples taken from the literature. We considered two possible riverine end-members: (1) the average unaltered riverine water (weighted using NL-DOC concentrations and riverine discharge rates); and (2) the average photobleached riverine NL-DOM (on average 1.48 ‰ more enriched than the unaltered riverine NL-DOM). The shift in $\delta^{13}C_{NL\text{-}DOC}$ between the unaltered and photobleached riverine end-members is statistically different at a 99 % confidence interval ($t_d = 3.37 > 3.25$). We recalculate the terrestrial component of mid-ocean NL-DOC (Druffel et al., 1992) and obtain relative contributions ranging between 6 and 32 % using the new, photobleached riverine $\delta^{13}C$ value, which amplifies the terrestrial signal in oceanic DOC by 22 % compared to the $\delta^{13}C$ signature of unaltered riverine water.

As an example, if oceanic DOC is calculated to contain a 30 % terrestrial component, only about 15 % of each river's NL-DOC discharge would have to be incorporated into the slow cycling oceanic DOC pool to account for this terrestrial contribution, which likely is the residual, most recalcitrant fraction of the global riverine DOC (this calculation assumes that the turnover time of the terrestrial oceanic component of oceanic DOC is similar to that of bulk oceanic DOC). This low value is consistent with the exhaustiveness of the photobleaching and other removal processes for terrestrial DOM (Table 1).

The scarceness of lignin and the $\delta^{13}C$ range allowed for marine DOM have previously precluded a terrestrial DOC component of any significance in the open-ocean (Williams and Druffel, 1987). However, the breadth and extent of chemical reactions that alter riverine DOC also affect our ability to molecularly characterize the overall composition of DOM and to identify specific terrestrial proxies. This work is instrumental in constraining photochemically-induced shifts in $\delta^{13}C_{NL\text{-}DOC}$ signatures, providing

BGD
10, 17117–17144, 2013

geochemists with critical information for determining the source and reactivity of different components of oceanic DOM. Accounting for $\delta^{13}C$ shifts also allows tracking more efficiently the transfer of organic matter from land to sea, which is a key link in the global carbon cycle, providing the most important pathway for ultimate preservation of terrigenous production (Hedges, 1992). Along with new proxies, methods and computer simulations designed to track terrestrial DOM in the oceans, our results contribute to the on-going effort to further elucidate the addition and removal processes of DOM during the turnover of oceanic waters.

Acknowledgements. The authors would like to thank all the scientists who contributed to sampling for the Big River project: E. M. Paolucci (Parana), D. E. Musibono (Congo), A. Shantz (Mekong), S. R. Khan (Ganges-Brahmaputra), Q. Huang (Yangtze), W. Schneider (Lena), A. Rivas and C. E. Rezende (Amazon), E. Petrescu (Danube), and H. E. Reader (Mississippi) for organizing the collection of water samples. We thank Paul Middlestead, Dan Duru and Graham Hughes for their instrument expertise, Ville Kasurinen for epifluorescence microscopy and Hanna Aarnos for her help in conducting the experiments. This work was supported by grants (Y. G. and A. V.) and scholarships (K. L.) from NSERC, CFI, FQRNT and the Academy of Finland.

References

Aarnos, H., Ylöstalo, P., and Vähätalo, A. V.: Seasonal phototransformation of dissolved organic matter to ammonium, dissolved inorganic carbon, and labile substrates supporting biomass across the Baltic Sea, J. Geophys. Res., 117, G01004, doi:10.1029/2010JG001633, 2012.

Beaupré, S. R. and Druffel, E. R. M.: Photochemical reactivity of ancient marine dissolved organic carbon, Geophys. Res. Lett., 39, 39, L18602, doi:10.1029/2012GL052974, 2012.

Benner, R., Biddanda, B., Black, B., and McCarthy, M.: Abundance, size distribution, and stable carbon and nitrogen isotopic compositions of marine organic matter isolated by tangential-flow ultrafiltration, Mar. Chem., 57, 243–264, 1997.

Blough, N. V. and Del Vecchio, R.: Chromophoric DOM in the coastal environment, in: Biogeochemistry of Marine Dissolved Organic Matter, edited by: Hansell, D. A., and Canfield, D. E., Elsevier, San Diego, 509–540, 2002.

BGD
10, 17117–17144, 2013

Bouillon, S., Yambélé, A., Spencer, R. G. M., Gillikin, D. P., Hernes, P. J., Six, J., Merckx, R., and Borges, A. V.: Organic matter sources, fluxes and greenhouse gas exchange in the Oubangui River (Congo River basin), Biogeosciences, 9, 2045–2062, doi:10.5194/bg-9-2045-2012, 2012.

Cauwet, G.: DOM in the coastal zone, in: Biogeochemistry of Marine Dossolved Organic Matter, edited by: Hansell, D. A., and Carlson, C. A., Elsevier, San Diego, 579–602, 2002.

Chin-Leo, G. and Benner, R.: Enhanced bacterioplacton production and respiration at intermediate salinities in the Mississippi River plume, Mar. Ecol.-Prog. Ser., 87, 87–103, 1992.

Dittmar, T., Whitehead, K., Minor, E. C., and Koch, B. P.: Tracing terrigenous dissolved organic matter and its photochemical decay in the ocean by using liquid chromatography/mass spectrometry, Mar. Chem., 107, 378–387, 2007.

Druffel, E. R. M., Williams, P. M., Bauer, J. E., and Ertel, J. R.: Cycling of dissolved and particulate organic matter in the open ocean, J. Geophys. Res., 97, 15639–15659, 1992.

Goni, M. A., Yunker, M. B., Macdonald, R. W., and Eglinton, T. I.: The supply and preservation of ancient and modern components of organic carbon in the Canadian Beaufort Shelf of the Arctic Ocean, Mar. Chem., 93, 53–73, 2005.

Gonsior, M., Peake, B. M., Cooper, W. T., D'Andrilli, J., and Cooper, W. J.: Photochemically induced changed in dissolved organic matter identified by ultrahigh resolution fourier transform iron cyclontron resonance mass spectrometry, Environ. Sci. Technol., 43, 698–703, doi:10.1021/es8022804, 2008.

Hansell, D. A., Carlson, C. A., Repeta, D. J., and Schlitzer, R.: Dissolved organic matter in the ocean: new insights stimulated by a controversy, Oceanography, 22, 52–61, 2009.

Hayes, J. M.: Fractionation of carbon and hydrogen isotopes in biosynthetis processes, Rev. Mineral. Geochem., 43, 225–277, 2001.

Hedges, J. I.: Global biogeochemical cycles: progress and problems, Mar. Chem., 39, 67–93, 1992.

Hedges, J. I. and Oades, J. M.: Comparative organic geochemistries of soils and marine sediments, Org. Geochem., 27, 319–361, 1997.

Helms, J. R., Stubbins, A., Ritchie, J. D., Minor, E. C., Kieber, D. J., and Mopper, K.: Absorption spectral slopes ratios as indicators of molecular weight, source and photobleaching of chromophoric dissolved organic matter, Limnol. Oceanogr., 53, 955–969, 2008.

BGD
10, 17117–17144, 2013

Hernes, P. J. and Benner, R.: Photochemical and microbial degradation of dissolved lignin phenols: Implications for the fate of terrigenous dissolved organic matter in marine environments, J. Geophys. Res., 108, 3291–3299, 2003.
Jaffé, P. R., Ding, Y., Niggemann, J., Vähätalo, A. V., Stubbins, A., Spencer, R. G. M., Campbell, J., and Dittmar, T.: Global charcoal mobilization from soils via dissolution and rivering transport to the oceans, Science, 340, 345–347, 2013.
Lønborg, C. and Álvarez-Salgado, X. A.: Recycling versus export of bioavailable dissolved organic matter in the coastal ocean and efficiency of the continental shelf pump, Global Biogeochem. Cy., 26, GB3018, doi:10.1029/2012GB004353, 2012.
Lu, Y., Bauer, J. E., Canuel, E. A., Yamashita, Y., Chambers, R. M., and Jaffé, P. R.: Photochemical and microbial alteration of dissolved organic matter in temperate headwater streams associated with different land use, J. Geophys. Res., 118, 566–580, doi:10.1002/jgrg.20048, 2013.
Maher, D. and Eyre, B. D.: Insights into estuarine benthic dissolved organic carbon (DOC) dynamics using δ^{13}C-DOC values, phospholipid fatty acids and dissolved organic nutrient fluxes, Geochim. Cosmochim. Ac., 75, 1889–1902, 2011.
Meyers-Schulte, K. J. and Hedges, J. I.: Molecular evidence for a terrestrial component of organic matter dissolved in ocean water, Nature, 321, 61–63, 1986.
Miller, W. L. and Zepp, R. G.: Photochemical production of dissolved inorganic carbon from terrestrial organic matter: significance to the oceanic organic carbon cycle, Geophys. Res. Lett., 22, 417–420, 1995.
Milliman, J. D. and Farnsworth, K. L.: River Discharge to the Coastal Ocean – a Global Synthesis, 1st edn., Cambridge University Press, 2011.
Mopper, K., Zhou, X., Kieber, D. J., Sikorski, R. J., and Jones, R. N.: Photochemical degradation of dissolved organic carbon and its impact on oceanic carbon cycle, Nature, 353, 60–62, 1991.
Moran, M. A., Sheldon Jr., W. M., and Zepp, R. G.: Carbon loss and optical property changes during long-term photochemical and biological degradation of estuarine dissolved organic matter, Limnol. Oceanogr., 45, 1254–1264, 2000.
Nelson, N. B., Siegel, D. A., Carlson, C. A., and Swan, S. M.: Tracing global biogeochemical cycles and merional overturning circulation using chromophoric dissolved organic matter, Geophys. Res. Lett., 37, L03610, doi:10.1029/2009GL042325, 2010.

BGD
10, 17117–17144, 2013

Obernosterer, I. and Benner, R.: Competition between biological and photochemical processes in the mineralization of dissolved organic carbon, Limnol. Oceanogr., 49, 117–124, 2004.
Ogawa, H. and Tanoue, E.: Dissolved organic matter in oceanic waters, J. Oceanogr., 59, 129–147, 2003.
Opsahl, S. and Benner, R.: Distribution and cycling of terrigenous dissolved organic matter in the ocean, Nature, 386, 480–482, 1997.
Opsahl, S. and Zepp, R. G.: Photochemically-induced alteration of stable carbon isotope ratios in terrigenous dissolved organic carbon, Geophys. Res. Lett., 28, 2417–2420, 2001.
Osburn, C. L., Morris, D. P., Thorn, K. A., and Moeller, R. E.: Chemical and optical changes in freshwater dissolved organic matter exposed to solar radiation, Biogeochemistry, 54, 251–278, 2001.
Panetta, R. J., Ibrahim, M., and Gélinas, Y.: Coupling a high-temperature catalytic oxidation total organic carbon analyzer to an isotope ratio mass spectrometer to measure natural-abundance δ^{13}C-dissolved organic carbon in marine and freshwater samples, Anal. Chem., 80, 5232–5239, 2008.
Pullin, M. J., Bertilsson, S., Goldstone, J. V., and Voelker, B. M.: Effects of sunlight and hydroxyl radical on dissolved organic matter: bacterial growth efficiency and production of carboxylic and other substrates, Limnol. Oceanogr., 49, 2011–2022, 2004.
Raymond, P. A. and Bauer, J. E.: DOC cycling in a temperate estuary: a mass balance approach using natural ^{14}C and ^{13}C isotopes, Limnol. Oceanogr., 46, 655–667, 2001a.
Raymond, P. A. and Bauer, J. E.: Riverine export of aged organic matter to the North Atlantic Ocean, Nature, 409, 497–499, 2001b.
Rossel, P. E., Vähätalo, A. V., Witt, M., and Dittmar, T.: Molecular composition of dissolved organic matter from a wetland plant (Juncus effusus) after photochemical and microbial decomposition (1.25 yr): common features with deep sea dissolved organic matter, Org. Geochem., 60, 62–71, 2013.
Spencer, R. G. M., Stubbins, A., Hernes, P. J., Baker, A., Mopper, K., Aufdenkampe, A. K., Dyda, R. Y., Mwamba, V. L., Mangangu, A. M., Wabakanghanzi, J. N., and Six, J.: Photochemical degradation of dissolved organic matter and dissolved lignin phenols from the Congo River, J. Geophys. Res., 114, 1–12, 2009.
Stutter, M. I., Richards, S., and Dawson, J. C. C.: Biodegradability of natural dissolved organic matter collected from a UK moorland stream, Water Res., 47, 1169–1180, 2013.

BGD
10, 17117–17144, 2013

Vähätalo, A. V. and Wetzel, R. G.: Long-term photochemical and microbial decomposition of wetland-derived dissolved organic matter with alteration of $^{13}C : ^{12}C$ mass ratio, Limnol. Oceanogr., 53, 1387–1392, 2008.

Vähätalo, A. V., Salonen, K., Salkinoja-Salonen, M., and Hatakka, A.: Photochemical mineralization of synthetic lignin in lake water indicates enhanced turnover of aromatic organic matter under solar radiation, Biodegradation, 10, 415–420, 1999.

Vähätalo, A. V., Salonen, K., Münster, U., Järvinen, M., and Wetzel, R. G.: Photochemical transformation of allochtonous organic matter provides bioavailable nutrients in a humic lake, Arch. Hydrobiol., 156, 287–314, 2003.

Vähätalo, A. V., Aarnos, H., Hoikkala, L., and Lignell, R.: Photochemical transformation of terrestrial dissolved organic matter supports hetero-and autotrophic production in coastal water, Mar. Ecol.-Prog. Ser., 423, 1–14, 2011.

Vodacek, A., Hogel, F. E., Swift, R. N., Yungel, J. K., Peltzer, E. T., and Blough, N. V.: The use of in situ and airborne fluorescence measurements to determine UV absorption coefficients and DOC concentrations in surface waters, Limnol. Oceanogr., 40, 411–415, 1995.

Williams, P. M. and Druffel, E. R. M.: Radiocarbon in dissolved organic matter in the central North Pacific Ocean, Nature, 330, 246–248, 1987.

Xiao, Y.-H., Sara-Aho, T., Hartikainen, H., and Vähätalo, A. V.: Contribution of ferric iron to light absorption by chromophoric dissolved organic matter, Limnol. Oceanogr., 58, 653–662, 2013.

Yu, J., Elderfield, H., and Piotrowski, A. M.: Seawatercarbonate ion-$\delta^{13}C$ systematics and applications to glacial-interglacial North Atlantic ocean circulation, Earth Planet. Sc. Lett., 271, 209–220, 2008.

Zepp, R. G.: Light and environmental chemistry: influence of changing solar radiation on aquatic photoreactions, IUVA News, 7, 9–14, 2005.

BGD
10, 17117–17144, 2013

Table 1. Concentration and $\delta^{13}C$ of various NL-DOC reactivity classes for each riverine sample. Standard deviations are given in brackets. $\delta^{13}C$ values are not given when NL-DOC concentrations were below 1 mg L^{-1}, due to the poor reproducibility of these measurements. The initial NL-DOC concentrations and $\delta^{13}C$ are obtained after storage and transportation of unfiltered and unpreserved samples, allowing the removal of the L-DOC component prior to this measurement. The Amazon River was sampled at two locations upstream of the confluence point of Rio Negro and Rio Solimoes. Samples from the two locations were mixed in an appropriate ratio (1 : 3 Rio Negro to Rio Solimoes) to represent the bulk riverine discharge. The percentage of photodegraded and microbially degraded NL-DOC represents the losses of NL-DOC occurring each of these processes and average values are normalized to discharge rates (Cauwet, 2002) and NL-DOC concentrations.

River name	Latitude	Longitude	Discharge rate	NL-DOC		Photooxidation		Microbial degradation	
					$\delta^{13}C$		$\delta^{13}C$ of residual		$\delta^{13}C$ of residual
			($km^3 yr^{-1}$ or $10^{12} L yr^{-1}$)	(mg L^{-1})	(‰)	(% loss)	(‰)	(%)	(‰)
Amazon	03°08′00″ S	59°54′10″ W	5780	4.00	−28.99	37.4	−27.45	33.0	−27.4
				(0.12)	**(0.17)**	**(0.7)**	**(0.05)**	**(3.0)**	**(0.3)**
Danube	45°13′38″ N	28°44′05″ E	198	2.30	−28.36	33.5	−27.00	33.1	**n.a.**
				(0.02)	**(0.21)**	**(4.2)**	**(0.17)**	**(0.3)**	
Yangtze	31°45′49″N	121°2′22″E	925	1.74	−27.59	34.5	−27.11	28.7	**n.a.**
				(0.03)	**(0.36)**	**n.a.**	**n.a.**	**(0.6)**	
Congo	04°18′18″ S	15°28′32″ E	1300	5.94	−27.06	43.4	−25.36	37.7	−26.2
				(0.14)	**(0.23)**	**(0.1)**	**(0.53)**	**n.a.**	**n.a.**
Parana	34°18′07″ S	58°32′47″ W	470	2.95	−26.97	30.9	−24.05	28.7	−26.5
				(0.00)	**(0.03)**	**(2.1)**	**(0.05)**	**n.a.**	**n.a.**
Lena	71°54′14″ N	127°15′16″ E	505	5.35	−26.87	29.6	−25.41	25.0	−25.5
				(0.22)	**(0.14)**	**(1.8)**	**(0.07)**	**(0.0)**	**(0.0)**
Mississippi	29°02′20″ N	89°19′20″ W	410	3.40	−26.58	25.1	−25.69	31.7	**n.a.**
				(0.08)	**(0.11)**	**(2.1)**	**(0.38)**	**(1.6)**	
Ganges-Brahmaputra	23°34′12″N	90°10′54″E	971	0.79	−26.49	34.0	−25.84	21.9	**n.a.**
				(0.03)	**(0.94)**	**(4.4)**	**(0.36)**	**(2.07)**	
St. Lawrence	46°54′45″ N	70°52′32″ W	413	3.55	−26.13	16.0	−25.47	31.9	−25.2
				(0.10)	**(0.16)**	**n.a.**	**n.a.**	**(0.8)**	**(0.0)**
Mekong	11°33′28″ N	104°56′53″ E	666	1.40	−25.98	16.6	−24.52	25.1	**n.a.**
				(0.12)	**(0.21)**	**n.a.**	**n.a.**	**n.a.**	
Weighed average				**3.60**	**− 28.07**	**35.9**	**− 26.57**	**32.56**	
				(0.1)	**(0.20)**	**(1.77)**	**(0.15)**	**(2.45)**	

n.a.= not available

BGD
10, 17117–17144, 2013

Table 2. Average end-member $\delta^{13}C$ values for 2 end-member mixing model and calculated riverine contributions for literature $\delta^{13}C$ values. The average riverine end-member is taken as either unaltered riverine water (−28.11 ‰) or photooxidized riverine water (−26.63 ‰). The algal end-member (−20.00 ‰) is taken from a theoretical 19 ‰ fractionation from dissolved DIC in the ocean (Bauer, 2002; Yu et al., 2008).

Study	Sample location	$\delta^{13}C$ ‰	% Riverine contribution Using unaltered $\delta^{13}C$	Using photobleached $\delta^{13}C$
(Raymond and Bauer, 2001a)	Mouth of the York River	−24.6	56.5	69.3
			(12,2)	**(9.9)**
(Druffel et al., 1992)	North Central Pacific Ocean most depleted $\delta^{13}C$	−22.1	25.8	31.6
			(5.6)	**(4.5)**
	North Central Pacific Ocean most enriched $\delta^{13}C$	−20.4	4.9	6.0
			(1.1)	**(0.8)**
(Panetta et al., 2008)	Lower St. Lawrence Estuary (5 m)	−24.5	55.3	67.9
			(11.9)	**(9.69)**
	Lower St. Lawrence Estuary (350 m)	−22.0	24.6	30.1
		−21.8	**(5.3)**	**(4.3)**
	Deep Sargasso Sea		22.1	27.1
			(4.8)	**(3.9)**
(Druffel and Bauer, 2000)	Southern Ocean	−21.7	20.9	25.6
			(4.5)	**(3.7)**
		−21.3	16.0	19.6
			(3.4)	**(2.8)**

BGD
10, 17117–17144, 2013

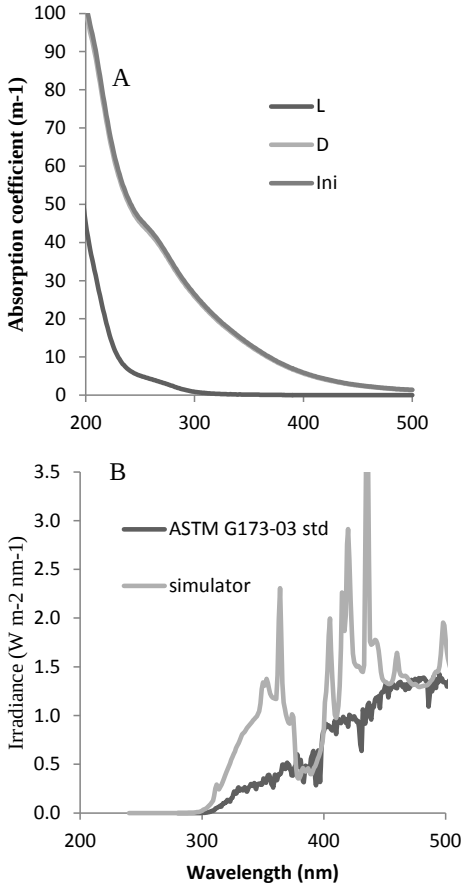

Fig. 1. Absorption coefficients of chromophoric dissolved organic matter in the initial (Ini), the irradiated (L) and the dark control (D) of Amazon River (A) and the spectral irradiance of solar simulator (simulator) and natural solar radiation (ASTM G173-03 std, Chu and Liu 2009; **(B)**. Note that the absorption spectra for Ini and *D* are almost perfectly superimposed in **(A)**.

BGD
10, 17117–17144, 2013

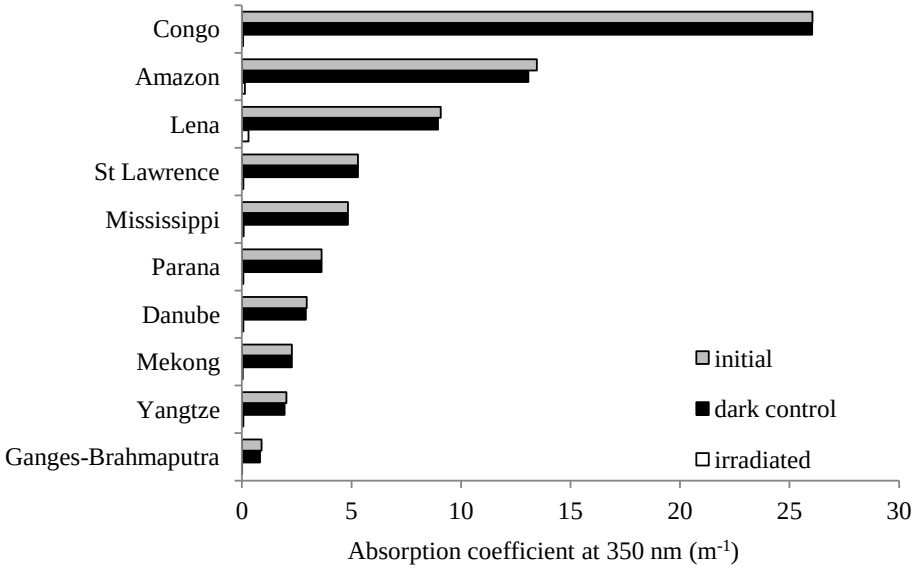

Fig. 2. Absorption coefficient of chromophoric DOM at 350 nm in the samples before (initial, grey) and after irradiation experiment in the irradiated (white) and the dark controls (black).

BGD
10, 17117–17144, 2013

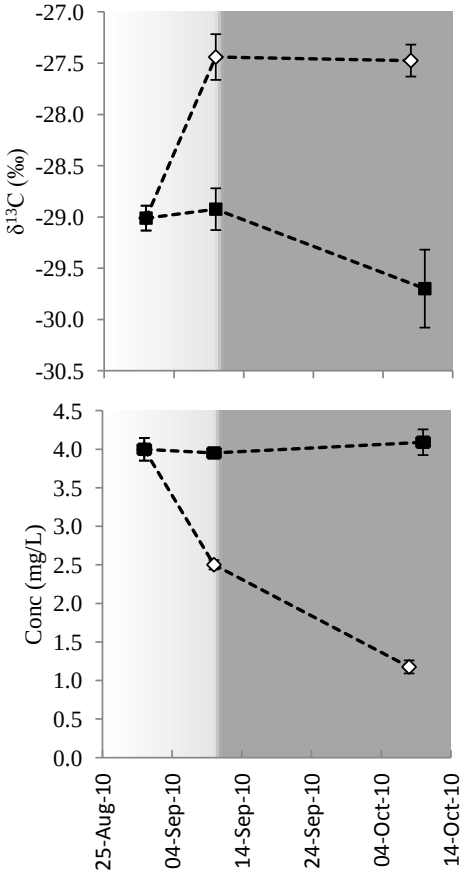

Fig. 3. Concentration of NL-DOC and its δ^{13}C value in a representative riverine sample during the 10 day abiotic photooxidation and the following 30 day microbial degradation initiated by inoculation with unfiltered riverine water containing indigenous bacteria. Irradiated samples are shown in white, while the dark controls are shown in black.

BGD
10, 17117–17144, 2013

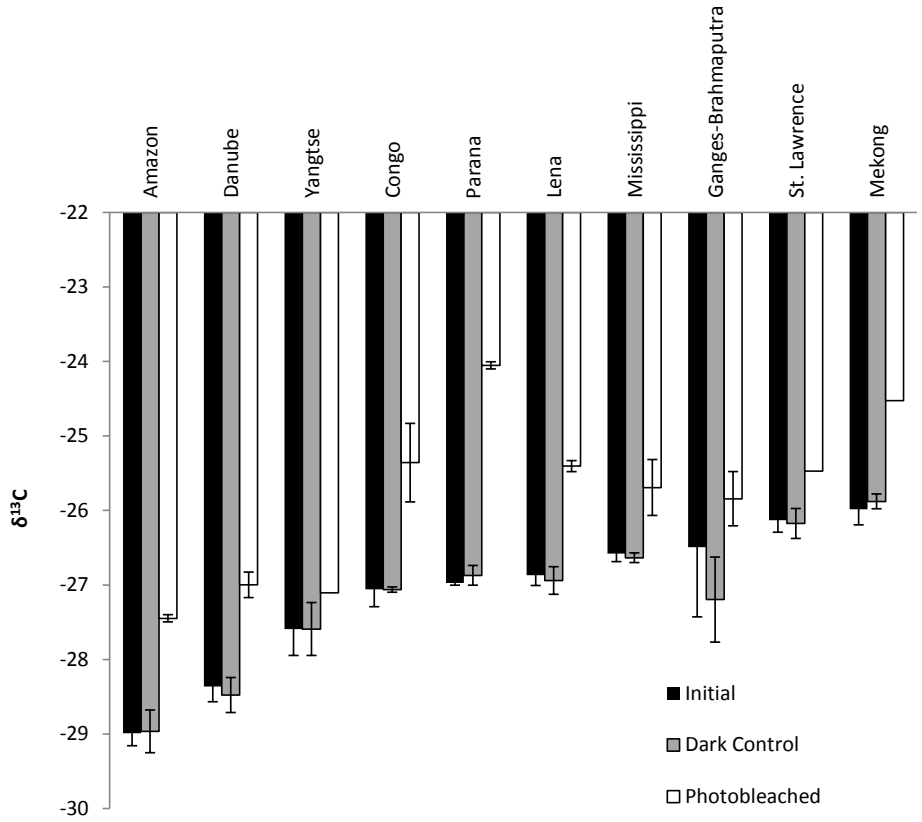

Fig. 4. Change in NL-DOC isotopic signature (δ^{13}C) as a result of photodegradation.

BGD
10, 17117–17144, 2013

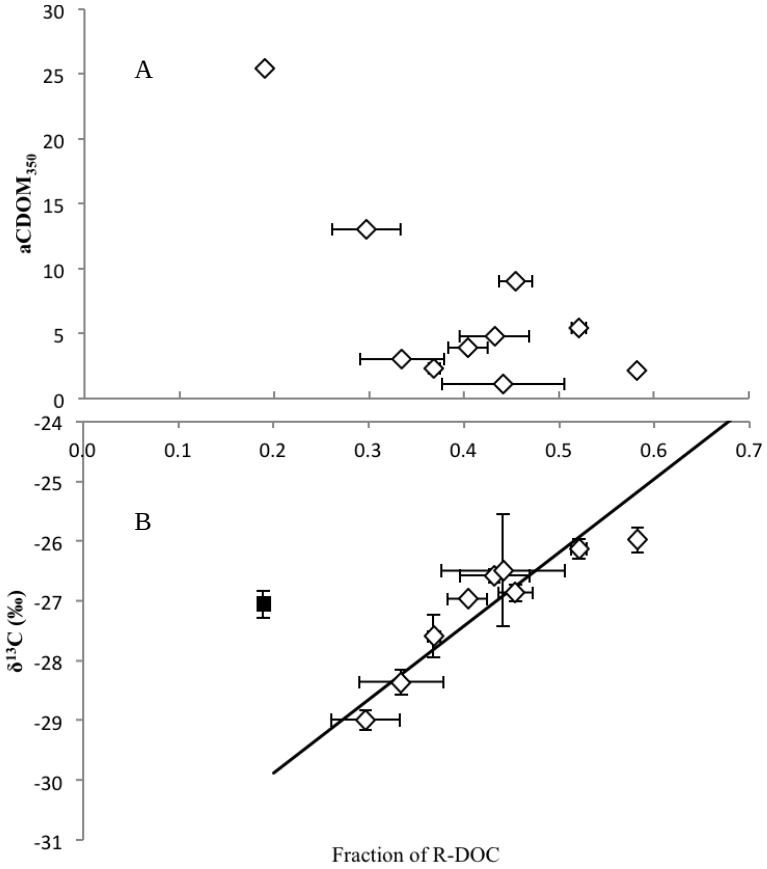

Fig. 5. Fraction of NL-DOC resistant to photooxidation followed by bacterial incubation (Recalcitrant DOC, R-DOC) as a function of the $\delta^{13}C$ signature of NL-DOC **(A)**, and the absorption coefficient at 350 nm **(B)** for all riverine samples. The error bars in **(A)** represent the propagated uncertainty for the fraction of NL-DOC remaining following the two treatments. The trendline describes a Model II linear regression model including all data except the Congo River.

BGD
10, 17117–17144, 2013